Short Communcation

Study on Electrochemical Corrosion Behavior of Co Base Super-alloys in Chloride Solution

Jiao-jiao Zhu[1], Li Feng[2], Jian-jun Guan[1], Peng Gao[1,], Xiao-ai Shi[3]*

[1] School of Mechanical Engineering, Liaoning Petrochemical University, Fushun 113001, Liaoning, China
[2] School of Electrical Engineering, Shengyang Polytechnic College, Shenyang 110045, China
[3] The Eighth Construction Company of CNPC Ltd., Fushun 113006, China
*E-mail: gaopeng@lnpu.edu.cn

The Co base super-alloys after heat treatment were studied, and its corrosion resistance in chlorine solution was evaluated by electrochemical methods. The surface morphology of Co base super-alloys was observed by Scanning Electron Microscope (SEM) before and after corrosion property tests. Potentiodynamic polarization and electrochemical impedance spectroscopy (EIS) were used to study electrochemical corrosion behavior of Co base super-alloys in chlorine solution. The results show that the typical μ phase is found after the heat treatment of the Co base super-alloys, and the μ phase appears as a light gray blocky morphology. The results of potentiodynamic polarization and EIS experiments show that the Co base super-alloys have the characteristics of a typical passivation metal. The potentiodynamic polarization experiment results show that the passivation range is -0.3V to 0.4V. The observation of the surface morphology shows that the μ phase of the Co base super-alloys has severe pitting corrosion. The corrosion not only expands along the substrate around the μ phase to form a groove, but also the corrosion holes continue to penetrate into the substrate and present a spiral shape.

1. INTRODUCTION

Cobalt is one of the transition metals that appear between iron and nickel. It was discovered by Brandt in 1735. Cobalt, chromium, carbon and tungsten elements make up a variety of alloys. These alloys are used in anti-wear, impact and severely corrosive environments. When you use it, it will contact with the elements such as S, K, Na and other elements. These elements react chemically with oxygen and NaCl. It will accelerate the corrosion of the alloy and cause the corrosion performance of the alloy to decrease. For example, the interaction of ships, gas turbines and fuels with the ocean and atmosphere leads to the electrochemical corrosion of the alloy caused by chloride salts on the alloy

Int. J. Electrochem. Sci., 16 **(2021)** Article ID: 210649

2

surface under the action of high temperature [1]. The main condition for pitting in electrochemical corrosion is the presence of corrosive anions. Corrosion will produce strong damage to the material, which has a great hidden danger. It could cause a catastrophic accident.

Co base super-alloys have excellent high temperature mechanical properties. Co base super-alloys are the main material for nozzle guide vane and guide vane of aerospace engine, naval gas turbine, industrial gas turbine, turbine blade and nuclear power plant [2-3]. Generally speaking, the best wear resistance of the alloy is due to the addition of a large amount of carbon, which leads to the formation of carbides in the alloy's microstructure during the solidification process. These carbides not only increase the hardness of the alloy and its resistance to stress wear. It also significantly improves the corrosion resistance and the ductility. Carbide strengthening has also been widely used in Co base super-alloys [4]. According to relevant reports, as-cast Co base super-alloys carbides mainly include M_7C_3, MC, M_6C and $M_{23}C_6$ [5]. The stability of the primary phase M_7C_3 carbide is the lowest. At high temperature, M_7C_3 precipitates fine secondary carbides $M_{23}C_6$. When the temperature reaches a certain limit, the fine secondary carbide $M_{23}C_6$ slowly transforms into the stable state of M_7C_3 type carbide. MC type carbides are the most stable [5].

The purpose of heat treatment of Co base super-alloys is to control the precipitation of carbides. The purpose of solid solution treatment is to dissolve all the primary carbides and some MC type carbides into the matrix solid solution. The aging treatment is to precipitate the carbide again. The fundamental reason for the superior corrosion resistance of Co base super-alloys is not clear. This article preliminarily studies the electrochemical corrosion mechanism of Co base super-alloys in chlorine solution after heat treatment. Mainly discuss the microstructure morphology of the Co base super-alloys after heat treatment, the passivation characteristics of the alloy and the microstructure after corrosion.

2. MATERIALS AND METHODS

2.1 Preparation and heat treatment of materials

Co base super-alloys are cast. Its chemical composition is shown in Table 1. The Co base super-alloys sample was cut routinely according to the electrochemical test requirements. Use KSL1700X heat treatment high temperature box furnace for heat treatment of experimental samples. Firstly, the solution treatment was carried out at 1200℃ for 4 hours and then air cooled. After aging treatment, it was held at 950℃ for 12 hours before air cooling.

Table1. Chemical composition of Co base super-alloys (wt.%)

Co	W	Ni	Cr	Ta	Hf	Ti	C	B	Mo	Al
Bal.	10	30	5.0	8.0	1.5	2.0	0.05	0.024	5.0	4.0

*2.2 Microstructure characterization of Co base super-alloys*

The surface morphology of Co base super-alloys after corrosion was characterized by SEM. Electrochemical corrosion behavior of Co base super-alloys in chloride solution was investigated by potentiometric polarization and electrochemical impedance spectroscopy (EIS). Electrochemical measurements were carried out at room temperature in Shanghai Chen Hua Instrument Electrochemical Workstation.

2.3 Experimental process

The sample material is cast Co base super-alloys. The samples of Co base super-alloys are routinely cut according to the experimental requirements. The sample for the electrochemical corrosion test is a circular sheet with a diameter of 10mm and a thickness of 1.5mm. The cut sample will be heat treated. After the heat treatment, a series of silicon carbide grinding paper was used to mechanically grind the samples to 2000 grains of sand. Use diamond polishing paste for polishing. To obtain the mirror finish required for metallographic analysis. Use alcohol for degreasing and ultrasonic cleaning for subsequent use. First, analyze the prepared samples by SEM and XRD patterns. Then do electrochemical experiments, and perform SEM microstructure analysis after completing each step of the electrochemical experiment. Graphite flakes are used as electrodes and saturated calomel is used as reference electrode. A sample with an area of 1 cm^2 is used as the working electrode. The mass fraction of NaCl electrolyte is 3.5%. Remove the passivation film on the surface of the working electrode before the potentiodynamic polarization and EIS experiment. The electrochemical measurement was carried out in the room temperature environment of the electrochemical workstation of Shanghai Chen Hua Instruments. After the sample is immersed in the chlorine solution, we wait for the open circuit potential to stabilize and then conduct the test. The sensitivity is set to -003, the potential is set to -0.3V, the time is set to 180s, the scan rate is 1 mv/s, and the scan range is -1.5 V ~ 3 V.

3. RESULTS AND DISCUSSION

We will study the as-cast super-alloys after heat treatment. The Co base super-alloys mainly composed of matrix and carbide. The SEM microstructure of the Co base super-alloys after heat treatment is shown in Figure 1.In the picture we clearly observe the typical μ phase. The μ phase appears as a light gray blocky morphology. The XRD pattern of the Co base super-alloys after heat treatment is shown in Figure 2. The XRD peak is only related to μ phase, and consists of a single μ phase. The morphology observed by SEM is consistent with that by XRD. As we all know, μ phase is a topological phase (TCP). The crystal structure is complex, including 13 diamond-shaped atomic cells. Its prototype is W_6Fe_7 [6-8]. The morphology of the μ phase by SEM is consistent with the typical μ phase result in reference [9].
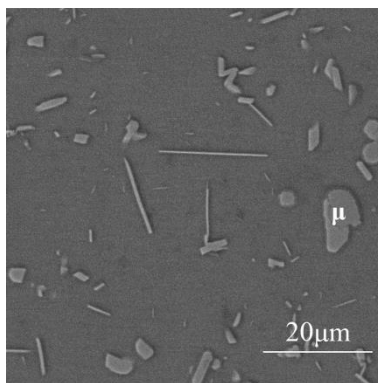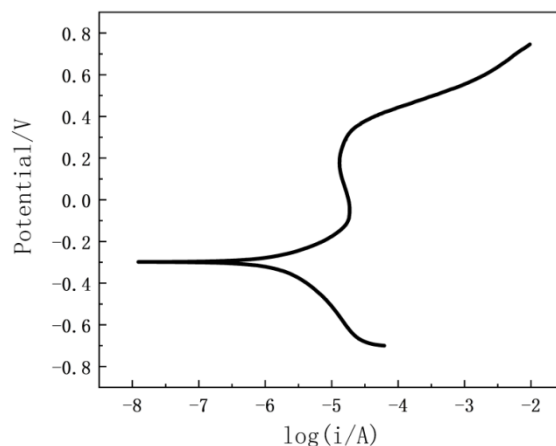
Figure 1. SEM micrograph of Co base super-alloys samples after heat treatment
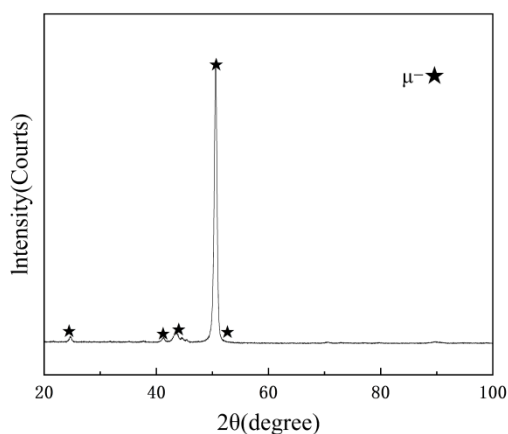
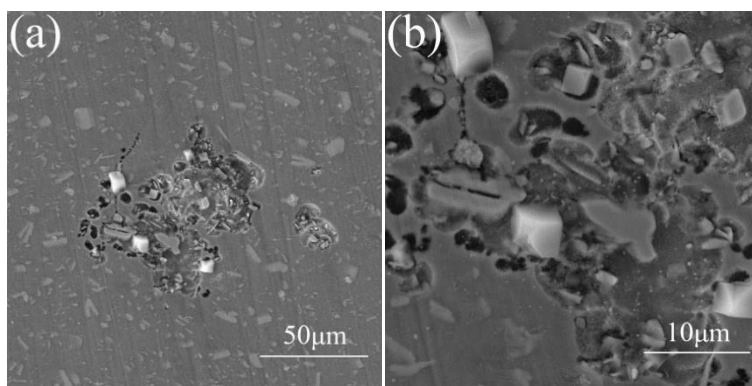**Figure 2.** XRD pattern of Co base super-alloys samples after heat treatment

3.1 Potentiodynamic polarization measurement

The polarization curve of the sample in chlorine solution is shown in Fig. 3. It can be seen from the curve that stable passivation has occurred. From the beginning of corrosion potential to -0.2V, the density of corrosion current shows a linear trend of increase, and the corrosion is constantly intensified. In the range of 0-0.2V, the polarization curve becomes relatively flat, and the corrosion rate of the Co base super-alloys is relatively low. In this region, the current density decreases with the increase of potential and the passivation platform appears on the curve. It indicates that passivation has occurred here.

Figure 3. Polarization curves of Co base super-alloys samples in chlorine solution

The SEM micrograph of the Co base super-alloys after polarization corrosion is shown in Figure 4. As shown in Figure 4(a), the appearance morphology shows that obvious pitting corrosion occurs on the surface of the alloy sample. Pitting holes are relatively independent and deep. Many pitting corrosions combine to form shallower localized corrosion morphology. According to reports, pitting corrosion always occurs in the presence of corrosive anions. The main cause of pitting corrosion is usually chloride ions. The electrolyte solution in our experiment is 3.5% NaCl, which meets the conditions for pitting corrosion. The composition and structural details of passivation play a minor role in the pitting process, but all alloys that undergo pitting corrosion have passivation properties. We also observed a stable passivation phenomenon in the polarization curve. From reference [10] we know that as the potential continues to increase, the current density continues to increase. The balance of the passivation film on the alloy surface will be broken. The rupture of the passivation film indicates that steady-state pitting occurs on the surface of the sample. We observed obvious pitting corrosion in the SEM microstructure. In the case of higher magnification, the pitting corrosion is clear, as shown in Figure (b). It can be observed from the figure that the surface of the alloy is partially dissolved. The pits are combined to form a groove, and the corrosion of the alloy further expands. Corrosion holes gradually spread to the inside of the alloy. Corrosion holes not only spread radially to the surroundings in the horizontal direction, but also continue to penetrate into the substrate in the vertical direction, forming deeper and larger pits.

Figure 4. SEM micrograph of Co base super-alloys samples after Potentiodynamic polarization measurement
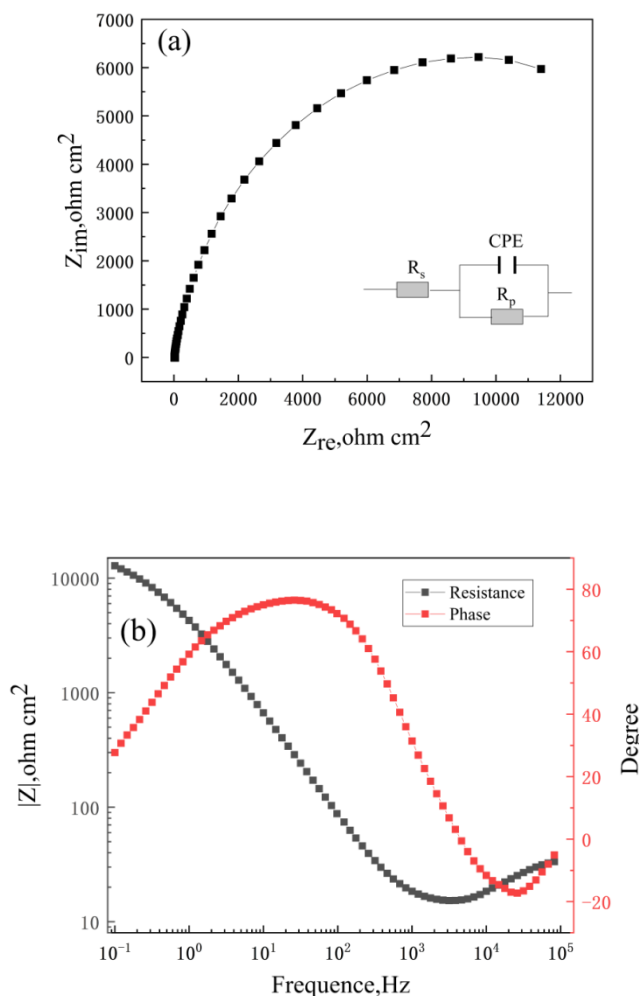
3.2 EIS measurement

The AC impedance spectrum of the sample of the Co base super-alloys in the chlorine solution is shown in Figure 5 (a). It is observed that the AC impedance spectrum presents a single capacitive reactance arc from the high frequency to the low frequency region, which has the characteristics of a typical passive metal impedance spectrum.

The surface of the alloy that undergoes an electrochemical reaction can be represented by an approximate circuit. When pitting corrosion exists on the surface of Co base super-alloys, the corresponding equivalent circuit can be expressed as a series circuit composed of resistors and components. It can be seen from the AC impedance diagram that there is only one capacitive reactance arc from the high frequency to the low frequency region. So the equivalent circuit of the electrochemical impedance spectrogram obtained in this experiment is R(QR) type. The equivalent circuit diagram matching the EIS spectrum is shown in 5 (a). The fitting results are shown in Table 2. Rs is the solution resistance, expressed as the electrolyte impedance between the reference electrode and the working electrode. Rp is the film resistance, which represents the film resistance of the corrosion products formed on the surface of the alloy. CPE is a capacitive element formed by the corrosive liquid and the working surface (It is not an ideal capacitive element) [11]. The fitting results are shown in Table 2. The values of the membrane resistance and the capacitive element are very low, which indicates that the membrane resistance of the corrosion products is very small. It does not increase the density of the oxide film.

The frequency resistance characteristic curve of the sample of Co base super-alloys in chlorine solution is shown in Figure 5 (b). In the high frequency region, the passivation film of the alloy exhibits a resistance behavior corresponding to the solution resistance between the working electrode and the reference electrode. In the low frequency range, the passive film of the alloy has capacitive behavior. The passivation film formed by the alloy in the low frequency region has obtained a certain impedance modulus.

The phase frequency characteristic curve of the Co base super-alloys sample in the chlorine solution is shown in Figure 5 (b). The corrosion resistance of the phase-frequency characteristic curve is generally determined by the phase angle. The phase-frequency characteristic curve in Figure 5 (b)

shows a one-time constant. In a wide frequency range, the maximum phase angle is 77°. This means that the alloy forms a stable passivation film [12].

Figure 5. EIS measurement: (a) The equivalent circuit diagram of AC impedance spectrum and AC impedance spectrum of Co base super-alloys, (b) The resistance frequency characteristic curve and phase frequency characteristic curve of Co base super-alloys

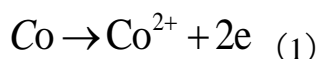**Table 2.** Fitting parameters of EIS test results

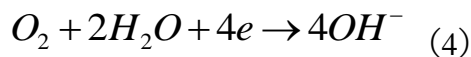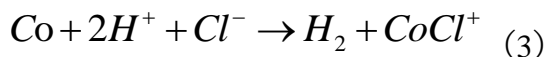| Solution concentration Cl⁻	3.5% NaCl
R_S	22.7
C	2.258E-5
R_P	1.199E-4

The SEM micrograph of the Co base super-alloys after EIS is shown in Figure 6. We can clearly observe in Figure (a) that the form of corrosion is mainly pitting, with obvious corrosion holes. The pitting corrosion mainly occurs in the μ phase. The morphology of the alloy observed at high magnification is clearer as shown in Figure (b). Corrosion began to appear black spots in the eroded area around the μ phase and the μ phase. The small dots are constantly combined with the pits. Along the periphery of the μ phase, the local topography of the alloy is corroded into uneven pits. The morphology of the alloy observed at higher magnification is shown in Figure (c). The black spots in the eroded area are more obvious. Moreover, the corrosion continues to deepen to form a groove, and the local corrosion becomes more serious. The morphology of corrosion is whirlpool. Corrosion continues to expand along the μ phase in the horizontal direction. In the vertical direction, the corrosion holes continue to penetrate into the substrate. The spiral shape continues to expand, forming deeper and larger pits.

Only the typical μ phase was found in this experiment, and no other strengthening phases were found. There are many factors that affect the corrosion of alloys, such as alloy crystal defects, metallographic structure, chemical composition and second equality [13]. As we all know, because of the secondary phase growth in the super-alloys structure, it is more susceptible to attack by the corrosive environment [14]. Research by Jos´e et al. showed that in the area, the area without chemical modification is more resistant to local corrosion. Because of the formation of the second phase, there is a gradient in the composition of the alloy. This area is more sensitive than the rest of the surface and dissolves faster. The material will be more prone to local corrosion [14]. This non-uniformity of the composition in the material microstructure promotes the formation of a non-uniform passivation film. The higher defect concentration and greater porosity make it easier for chloride ions to penetrate the layer. Chlorine is a strongly acidic anion. Many metal cations have considerable solubility in chlorine solution. Chloride ion is also a relatively small anion with a high diffusivity.

The main cause of pitting corrosion is generally chloride ions. At present, there are many mechanisms to explain the pitting corrosion of alloys caused by Cl^- [15-17]. Its "occluded corrosion cell" (Occluded Corrosion Cell, abbreviated as OCC) theory can well explain the pitting corrosion behavior of Co base super-alloys [18]. Occluded battery is formed at the defected surface of the Co base super-alloys. The elements such as Co and Al in the alloy are partially dissolved and undergo a hydrolysis reaction. Occluded battery is formed at the defected surface of the Co base super-alloys. The elements such as Co and Al in the alloy are partially dissolved and undergo a hydrolysis reaction. Reduce the internal PH of the occluded battery. In order to maintain the neutrality of the internal solution, OCC external anions migrate to the internal. Due to the high concentration of Cl^- and the small radius, it first diffuses to the outside of the OCC and preferentially forms compounds with metal ions.

Electrochemical corrosion reactions similar to Ni-based super-alloys mainly occur inside OCC.

$$Co \rightarrow Co^{2+} + 2e \quad (1)$$

$$Co^{2+} + 2H_2O \rightarrow Co(OH)_2 + 2H^+ \quad (2)$$

$$Co + 2H^+ + Cl^- \rightarrow H_2 + CoCl^+ \quad (3)$$

$$O_2 + 2H_2O + 4e \rightarrow 4OH^- \quad (4)$$

As the chemical reaction continues, the pH value of the OCC internal solution gradually decreases. The corrosion hole is always in an active state, and the corrosion hole is continuously dissolved as an anode. Passivation occurs on the outside, and a reduction reaction of dissolved oxygen occurs at the cathode.

$$O_2 + 2H_2O + 4e \rightarrow 4OH^- \quad (5)$$
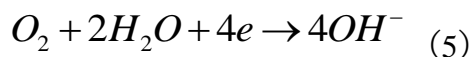
This activation-passivation battery system expands pitting corrosion. The energy spectrum elements at the edge of the inner wall of the etched hole are shown in Table 2. The analysis shows that Cl$^-$ is enriched around the corrosion hole. This is consistent with the above-mentioned theory that Cl$^-$ migrates to the inside of the etched hole and forms compounds with metal ions.
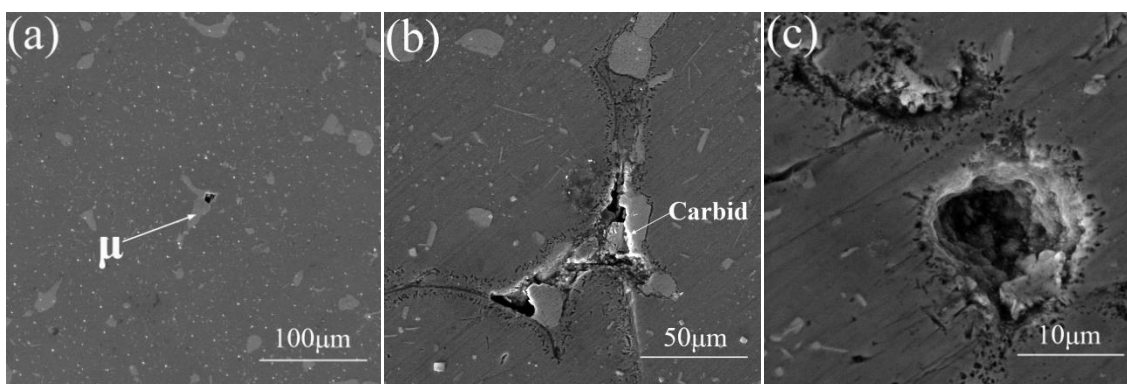
Figure 6. SEM micrograph of Co base super-alloys samples after EIS measurement

Table 3. The element table of the energy spectrum of the inner wall of the corrosion hole (%)

Cl	C	Co	Ni	Mo	Cr	Ta	Ti	Al	w
31.45	60.97	2.75	1.57	0.77	0.98	0.28	0.42	0.52	0.31

4.CONCLUSION

(1) After the heat treatment of the Co base super-alloys, the μ phase is found. It is presented as a light gray block structure.

(2)The results of polarization and EIS experiments show that the Co base super-alloys have the characteristics of a typical passivation metal. The polarization experiment results show that the passivation range is -0.3 to 0.4V.

(3) The observation of the surface morphology shows that the μ phase of the Co base super-alloys has severe pitting corrosion. The corrosion not only expands along the substrate around the μ phase to form a groove, but also the corrosion holes continue to penetrate into the substrate and present a spiral shape.

References

1. I.G. Akande, O.O. Oluwole, O.S.I. Fayomi, O.A. Odunlami, *Mater. Today*, 2021.
2. Juraj Belan, Lenka Kucharikova, Alan Vasko, Eva Tillova, *Mater. Today*, 4(2017) 5743-5748.
3. D. Prabhakaran,N.Jegadeeswaran, B. Somasundaram, B.S. Raju, *Mater. Today*, 20(2020)173-176.
4. Patrice Berthod, Lydia Toubal, *Mater. Chem. Phys*., 212(2018)260-267.
5. Weimin Gui, Hongyu Zhang, Min Yang, Tao Jin, Xiaofeng Sun, Qi Zheng, *J. Alloys Compd*., 728(2017)145-151.
6. L.R. Liu, B.X. Zhou, Q.F. Wang, Y.H. Yang, J.J. Yu, B.Z. Sun, *J. Alloys Compd*., 844(2020)155822.
7. Yongxin Cheng, Guanglei Wang, Jide Liu, Lianlong He, *Scr. Mater*., 193(2021)27–32.
8. Bin Yin, Guang Xie, Langhong Lou, Jian Zhang, *Scr. Mater.,*173 (2019) 1–4.
9. J. Liu, J.J. Yu, Y.H. Yang, Y.Z. Zhou, X.F. Sun, *Mater. Sci. Eng. A*, 745(2019)404-410.
10. Robert A Rapp, Corros. Sci., 44(2002)209-221.
11. K. Daub, X. Zhang, L. Wang, Z. Qin, J.J. Noël, J.C. Wren, *Electrochim. Acta*, 56(2011)6661-6672.
12. A. Fattah-alhosseini, S. Vafaeian, *J. Alloys Compds*., 639(2015)301-307.
13. W.Y. Guo, J. Sun, J.S. Wu, *Mater. Charact.,* 60(2009)173-177.
14. José Henrique Alano, Renato Luiz Siqueira, Amanda Dantas de Oliveira, Guilherme dos Santos Vacchi, Carlos Alberto Della Rovere, Sebastião Elias Kuri, *Corros. Sci*., 177(2020)108965.
15. Roland Tolulope Loto, *J. Mater. Res. Technol.,* 8(2019)623-629.
16. Bokai Liao, Hongyu Cen, Zhenyu Chen, Xingpeng Guo,*Corros. Sci.,* 143(2018)347-361.
17. Arafat Toghan, M. M. Abou-krisha, F. H. Assaf, F. El-Sheref1, *Int. J. Electrochem. Sci*., 16(2021) 151044.
18. Gan Yang, Li Ying, Lin Haichao, *Corros. Sci*., 43(2001)397-411.